

# ENERGY AND MASS SPECTROSCOPY OF IONS AND NEUTRALS IN COLD PLASMA

Marijan Maček<sup>1,2\*</sup> Miha Čekada<sup>2</sup>

<sup>1</sup>University of Ljubljana, Faculty of Electrical Engineering, Ljubljana, Slovenia

<sup>2</sup>Jožef Stefan Institute, Ljubljana, Slovenia

**Key words:** polymer; PES; PET; PPS; PS; PP; PA6; PTFE; cellulose; oxygen; plasma; functionalization; surface activation; surface modification, XPS

**Abstract:** A very versatile method for plasma characterization is plasma energy and energy-resolved mass spectroscopy. By this method energy and mass distributions of ions and neutrals can be analyzed. Results obtained on two different triode ion plating systems with different magnetic confinement show a good correlation between the average energy of the particles bombarding the surface and the properties of the layer (texture, stress-free lattice parameter and in minor extend others such as microhardness and internal stress).

In both systems single and multiply charged ions of Ar and N<sub>2</sub> gas and the evaporated Ti were detected. The system with a strong magnetic field confinement exhibits higher plasma potential ( $U_p = 55$  V) under the standard deposition conditions, the peak ion energy is higher and the energy distribution is narrower than in the system without magnetic confinement ( $U_p = 12$  to  $35$  V). Mass-spectroscopic studies reveal, that the electron impact ionization of titanium,  $Ti^{n+} + e^- \rightarrow Ti^{(n+1)+} + 2e^-$ ,  $n = 0-3$ , within the electron beam with an energy above  $27.5$  eV is very effective. The probability for the multiple charged ions in this system is much higher than in the system without the magnetic confinement, so the population of  $Ti^{++}$  in this system is higher than that of  $Ti^+$ . Even the presence of  $Ti^{3+}$  and  $Ti^{4+}$  ions was confirmed experimentally.

An additional promising technique is also so called multiple ion detection (MID) which is very suitable for monitoring of different plasma assisted processes like etching and cleaning.

## Energijsko ločljiva masna spektroskopija ioniziranih in nevtralnih delcev v hladni plazmi

**Ključne besede:** energijsko ločljiva spektroskopija plazme, ionsko nanašanje, TiC; TiN; TiCN

**Izvleček:** Za okarakterizacijo plazme je zelo primerna metoda energijsko ločljive masne spektroskopije. Z njo lahko pridobimo podatke o energijski in masni porazdelitvi ionov in nevtralnih delcev. Rezultati dobljeni v dveh sistemih za ionsko nanašanje z različnimi magnetnimi poljema pokažejo na dobro ujemanje med povprečno energijo delcev, ki zadevajo površino in lastnostmi nanosenih plasti (tekstura, mrežni parametri v stanju brez notranjih napetosti in v manjši meri trdota in notranje napetosti).

V obeh sistemih so bili zaznani enojno in večkratno nabiti ioni Ar, N<sub>2</sub> in neparjevanega Ti. Sistem z močnim magnetnim poljem ima med standardnimi pogoji nanašanja višji plazemski potencial ( $U_p = 55$  V), kar se odraža v energijski porazdelitvi ionov z vrhom pri višjih energijah, sama porazdelitev pa je ožja kot v sistemu z šibkim magnetnim poljem ( $U_p = 12$  do  $35$  V). Masna spektroskopija pokaže, da je ionizacija titana,  $Ti^{n+} + e^- \rightarrow Ti^{(n+1)+} + 2e^-$ ,  $n = 0-3$ , znotraj elektronskega curka z energijo nad  $27.5$  eV zelo učinkovita. Verjetnost za večkratno ionizacijo je v sistemu z močnim magnetnim poljem mnogo večja kot v sistemu s šibkim magnetnim poljem. Zato je populacija ionov  $Ti^{++}$  mnogo višja kot enkrat nabitih ionov  $Ti^+$ . Zaznana je bila celo prisotnost ionov  $Ti^{3+}$  in  $Ti^{4+}$ .

Zelo obetavna tehnika za spremljanje plazemskih postopkov (jedkanje, čiščenje) pa je metoda MID (multiple ion detection), pri kateri spremljamo populacijo različnih ionov tekom samega procesa.

### 1 Introduction

Plasma assisted processes are gaining more and more attention due to its benefits. The temperatures involved in the process are lower; lower is also environmental pollution in some cleaning processes, and there is a greater possibility to tailor the process according to technology demands due to wider range of parameters involved in the reaction.

However, for a successful implementation of plasma assisted processes, the thorough knowledge of plasma status is of the crucial importance. The main methods, suitable for its characterization are:

- *electrostatic (Langmuire) probe* /1, 2/, which gives a valuable information about the plasma parameters such as: electron temperature ( $T_e$ ) and its energy distribution, plasma potential ( $U_p$ ) and densities of electrons and ions ( $n_e$ ,  $n_i$ ),
- *optical emission spectroscopy*, OES /1, 3/. The method is very suitable to monitor the plasma assisted processes "ex-situ". But it can provide the information on the light emitting species only.
- *energy resolved mass spectroscopy* /1, 4/. This is the only method which can give information about the energy and mass distribution of ions (positive and negative) as well as neutrals from the plasma. On the

\* This work was done during my stay at Jožef Stefan Institute

other hand, the method is a rather complicated and invasive one, since the spectrometer sampling orifice is protruding into the vacuum chamber.

In this paper, the applications of energy resolved mass spectroscopy during the all steps of a hard coating process based on Ti(C,N) in an triode ion plating system are given.

The hard coatings can be deposited by different PVD and CVD techniques, but ion plating, especially triode one, is a very common method. The advantage are high deposition rate and good mechanical properties of deposited films due to high ionization rate accompanied by high ion energy as it was shown also in our previous investigations [5, 6].

The coatings properties are related to the chemical composition and to the microstructure, and depend on the state of the surface before the deposition (heating and etching) as well on the deposition conditions which affect the state of the plasma during ion plating process. There are many studies depicting the influence of the bombardment by energetic particles (especially ions and also radicals) on to the film microstructure and consequently on to the film properties [5, 7, 10], but the understanding of plasma during a typical ion plating processes is not so clear, due to the complicated nature of interactions between hot electrons and reactive gas molecules even in a case of a relatively simple binary gas mixture of Ar + N<sub>2</sub>, not to mention a more complicated systems involving also a (hydro)carbon precursor (CH<sub>4</sub>, C<sub>2</sub>H<sub>2</sub>,...).

## 2 Experimental

### 2.1 Energy resolved mass spectroscopy

The energy-resolved mass spectrometer, such as Balzers PPM421, schematically shown in Fig. 1, is a differentially pumped device. The entry orifice (100 mm) is usually at the floating potential, or it can be biased or grounded if desired. The ions from the plasma are focused by the ion optics in the ion measuring mode, or they are deflected in the neutral measuring mode applying the appropriate potential.

Neutrals from the plasma are ionised in the crossed-beam electron ionisation chamber. The electron beam current equals about 0.20 mA at the pre-selected acceleration voltage up to 70 V. In the neutral-measuring mode the chamber is grounded, but its potentials follow the energy scan in the ion mode.

Ions from the plasma or from the ionisation chamber are subsequently filtered by the cylindrical mirror energy analyser with the resolution  $\sim 0.3$  eV and then pass through the quadrupole mass analyser with the resolution<sup>1</sup>  $m/Dm = 100$ . In the present set-up the ions are deflected for

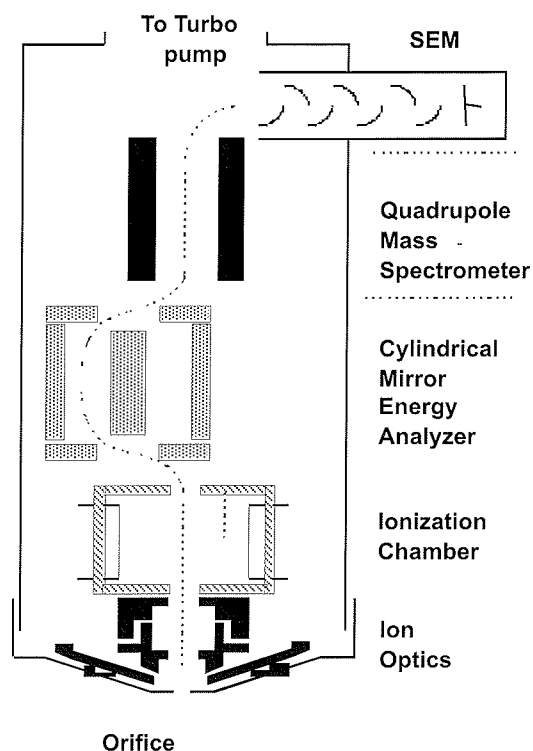


Fig. 1: Scheme of PPM421 energy and mass analyzer.

90° before they enter the secondary electron multiplier, where avalanche electrons are generated. In this way the sensitivity is greatly improved. It can give readings from  $10^{-1}$  to  $10^7$  counts per second (CPS).

The analyser can perform a mass scan at selected ion energy (mass spectrum), multiple ion detection (MID) at selected energy, or it can perform an energy scan at selected mass number  $m/q$ . The measured energy spectrum is actually a spectrum of stopping potential. Therefore, the real ion energy is the product of the measured stopping potential and the ion charge.

Under some conditions, especially when the mean free paths for charge-exchange and/or other collisions are comparable with the plasma sheath thickness, the measured energy distributions depend on the voltage applied on the extraction electrode. But for the most of experiments at relatively low pressures (below 0.5 Pa) the plasma has collision-free sheaths (sheath thickness  $d \ll 1$  mm, mean free path  $H \sim 20-40$  mm) and the measured distribution corresponds to the distribution in the plasma at least for the ions coming from the direction of the highest ion optics transmission.

An important problem arises since the spectrometer is partially immersed in the vessel with relatively strong magnetic field. Since it is very difficult to protect the whole spectrometer (inside and outside of the vacuum chamber with appropriate m-metal shield) from the effect of the magnetic field, we performed calibration measuring the effect of

<sup>1</sup>  $Dm$  is defined as the peak width at 10% of the maximum intensity

magnetic field on the spectra of neutrals. As to be expected only light ions ( $m/q < 12$  amu) are strongly affected. All our results for the integrals of ion intensities and energy distributions are corrected for the effect of the magnetic field. Mass spectra are as measured, therefore hydrogen ions ( $m/q = 1-3$  amu) are relatively underestimated for about 5-10 times regarding the peaks with  $m/q \geq 12$  amu.

## 2.2 Description of the system

Energy resolved mass spectrometry studies were performed in the commercial Balzers BAI 730 triode ion plating system. This system uses a filament-based ionisation chamber, which forms a low voltage (LV) arc expanding into the reaction chamber. The power supply is electrically floating with respect to the chamber walls

Its negative pole is connected to the arc cathode, while the positive one can be connected to different anodes, depending on the operation mode (heating, etching, and evaporation, /6/).

The standard deposition process for M(C,N) hard coatings in this system consists of 3 steps:

- *heating* with electrons in Ar plasma for about 60 min up to above 350°C
- *etching* of the substrate surfaces with Ar ions for 15 min to improve adhesion
- *deposition*.

The standard prescribed conditions for TiN ion plating are: arc current  $I_{arc} = 200$  A, substrate voltage  $U_B = -125$  V, argon pressure  $p_{Ar} = 0.15$  Pa (argon flow  $F_{Ar} \sim 90$  cm<sup>3</sup>/min), total pressure measured by ionisation gauge  $p_{tot} = 0.2$  Pa ( $F_{N_2} \sim 120$  cm<sup>3</sup>/min) and current in both coils  $I_C = 15$  A which corresponds to magnetic field of 7 mT measured at the centre of the vessel. A more detailed description of the system, effects of process parameters on to the plasma parameters deduced from the electrostatic probe measurements and energy resolved mass spectroscopy are given in /6, 11, 12/.

## 3 Results and discussion

### 3.1 Energy spectra of positive ions

The main advantage of the energy resolved mass spectroscopy is its ability to measure energy distribution of ions and neutrals. In Fig. 2a the energy spectrum of selected positive ions during TiN deposition under the standard conditions in the above described system is shown. The peak of the distribution at 55 eV corresponds to the measured plasma potential,  $U_{pl}$ . For comparison in Fig 2b the energy spectrum in a very similar ion plating system, but without magnetic confinement /5/, is shown. In this case the energy distribution is a wide one, spreading from 12 to about 35 eV, with Ar distribution centred at about 12 eV and Ti spread over the whole energy interval. Peaks of the energy distribution for this system correspond to the measured potentials in the system ( $U_{pl} = 15 - 35$  V) and are

positioned at a considerably lower energy than in the system with magnetic confinement, ( $U_{pl} = 55$  eV). Consequently the average energy  $\langle E \rangle$  and effective bias  $U_{eff}$  are lower than in the previous system.

Calculations in /5/ show that a difference of some -75 V in  $U_{bias}$  is necessary to get the same average particle energy in the system without magnetic confinement. The difference in the effective bias was confirmed by the relationship between the film properties (texture, stress-free lattice parameter and in minor extend others such as microhardness and internal stress).

### 3.2 Analysis of ion flux by mass spectroscopy

In Fig. 3 mass spectra measured during the deposition of Ti, TiN and TiC, i.e. in the working gas composed of Ar, Ar/N<sub>2</sub> and Ar/C<sub>2</sub>H<sub>2</sub> mixtures, respectively, are compared. Other parameters, the Ar pressure, corrected partial reactant pressure and arc current were the standard ones for TiN deposition.

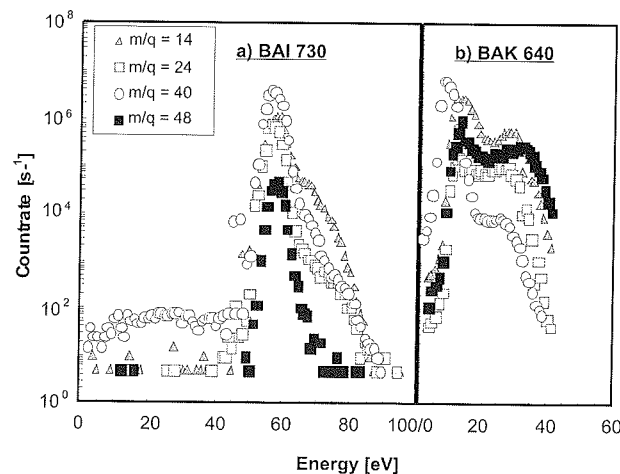


Fig. 2: Typical energy spectra of selected ions during deposition of TiN in two ion plating systems, a) with magnetic confinement, b) without magnetic confinement /5/

The mass spectrum for the Ti evaporation in pure Ar in Fig 3a reveals typical features of the plasma in the BAI 730 ion-plating apparatus /13/. A high degree of ionisation is notable for the evaporated Ti, highlighted by the fact that the intensities of the doubly charged  $Ti^{2+}$  ions observed at the mass-to-charge ratios from 23-25 are of the same order of magnitude as that of the singly charged  $Ti^+$  ions (peaks at  $m/q$  46-50 amu). There is even a well-defined peak of the triply charged  $Ti^{3+}$  ions centred at  $m/q = 16$  amu (not the oxygen  $O^+$ !), as shown in the insert, measured at higher resolution  $m/Dm$ . It is worth to note that we reported even on the presence of the ions  $Ti^{4+}$  with peaks centred at  $m/q = 12$  amu, but the intensity was about 100 times lower than that of  $Ti^{3+}$ . The Ar ions constitute the peaks at  $m/q = 40$  amu ( $Ar^+$ ) and 20 amu ( $Ar^{++}$ ). The peak

at  $m/q = 41$  amu ( $\text{ArH}^+$ ) is due to the contamination of the system with hydrogen during previous depositions.

When  $110\text{--}130\text{ cm}^3/\text{min}$  of nitrogen is added to the argon (equilibrium partial pressure  $p_{\text{N}_2} = 0.08$  Pa) strong peaks appear in the spectrum (Fig. 3b), in addition to those peaks discussed above. There are peaks at  $m/q = 14$  amu ( $\text{N}^+$  and/or  $\text{N}_2^{2+}$ ), at  $m/q = 28$  amu ( $\text{N}_2^+$ ), and at  $m/q = 7$  amu ( $\text{N}^{2+}$ ). The peak at 14 amu belongs, most probably, to  $\text{N}^+$  rather than  $\text{N}_2^{2+}$ , since the ratio of the intensities of the peaks at 14 amu and 28 amu is about 50. This is just the opposite to the ratio of about 0.02 between the doubly and the singly charged Ar ions at  $m/q = 20$  and 40 amu, respectively. In the spectrum one can also see some hydrogen and hydrocarbon contamination. The peaks at  $m/q = 15$  amu and 29 amu are hydrogenated nitrogen and argon, respectively, while the peak at  $m/q = 15$  amu could be  $\text{NH}^+$  and/or more probably  $\text{CH}_3^+$ , since it is accompanied by weaker peaks of the  $\text{CH}_{n=0-4}^+$  ion family.

Much more pronounced changes in mass spectrum (Fig. 3c) resulted after the addition of  $\text{C}_2\text{H}_2$  ( $85\text{--}90\text{ cm}^3/\text{min}$ , the same corrected partial pressure 0.08 Pa) to argon. In the previous case of ion plating in the Ar/ $\text{N}_2$  mixture only peaks belonging to N and  $\text{N}_2$  molecule appear. But now the spectrum contains many additional peaks as expected due to the complicated cracking pattern of the  $\text{C}_2\text{H}_2$  molecule. The most intense additional peak is at the mass number  $m/q = 41$  amu, which belongs to the hydrogenated argon ion  $\text{ArH}^+$ , followed by the hydrogen peaks at  $m/q = 1\text{--}3$  amu. The hydro-carbon ion intensities are relatively low, compared with nitrogen in the Fig. 3b. The most intense peak is the carbon peak at  $m/q = 12$  amu ( $\text{C}^+$  or  $\text{C}_2^{2+}$ ), while the hydrocarbon peaks  $\text{CH}_{n=1-4}^+$  and  $\text{C}_2\text{H}_{n=1-4}^+$  have an order of magnitude lower intensities, with the parent ion  $\text{C}_2\text{H}_2^+$  ( $m/q = 26$  amu) being the most intense of these.

However, it must be noted that the possibly present peaks at  $m/q = 24$  and 25 amu ( $\text{C}_2^+$ ,  $\text{C}_2\text{H}^+$ , respectively), could not be distinguished because of the strong contribution of the  $^{48,50}\text{Ti}^{2+}$  isotope ions at these mass numbers. But on the basis of our previous spectroscopic studies performed during CrC ion plating /14/ we believe that they are of lower intensity than the parent  $\text{C}_2\text{H}_2^+$  ion.

It is necessary to point out that the mass spectra are not corrected for the effect of magnetic field. It was already mentioned that hydrogen peaks are underestimated for about 5-10 times regarding the peaks with mass number  $m/q > 12$  amu, which are more or less insensitive to the magnetic field. Consequently, the intensity of the hydrogen peaks with  $m/q = 1\text{--}3$  amu is comparable to the intensity of the hydrogenated argon ion. The parent  $\text{C}_2\text{H}_2$  molecules are dissociated under the standard condition for the Ti evaporation ( $I_{\text{arc}} = 200$  A) almost to its single constituents, hydrogen and carbon. This is in agreement with observations in a hollow cathode arc deposition system /15/, where at the magnetic field comparable to that in our system the  $\text{C}^+$  ions appear to be the most abundant.

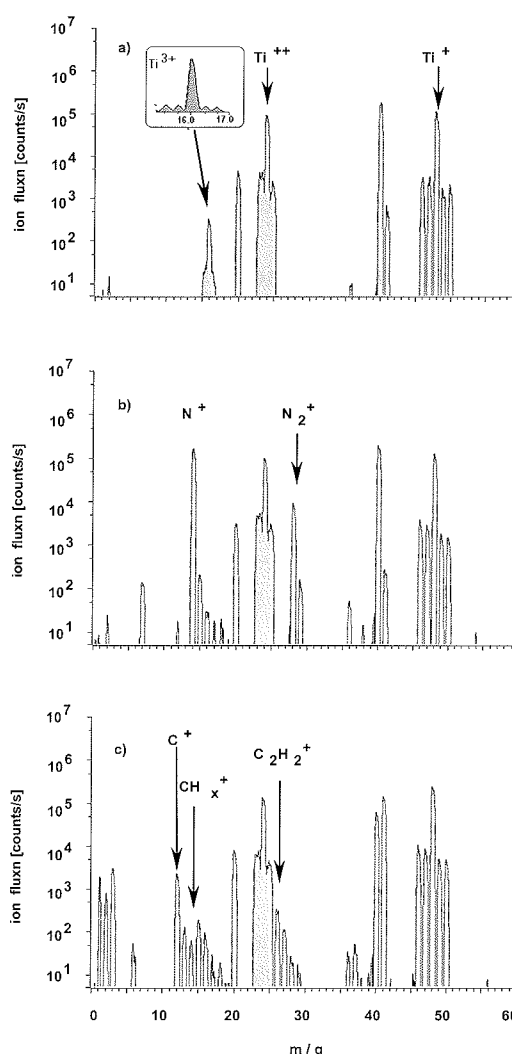


Fig. 3: Ion mass spectra measured during Ti evaporation at  $I_{\text{arc}} = 200$  A in pure argon (a), mixture of argon and  $120\text{ cm}^3/\text{min}$  nitrogen (b) and mixture of Ar and  $87\text{ cm}^3/\text{min}$  acetylene (c).

### 3.3 Mass spectra of the neutrals

The mass spectra of neutrals with near zero energy were measured using the ionisation source of the spectrometer ( $U = 70$  V) before ignition of the discharge and during the discharge with moderate  $I_{\text{arc}} = 175$  A. The mass spectrum in Fig. 4a is an example for the Ar/ $\text{C}_2\text{H}_2$  working gas mixture at low acetylene partial pressure,  $p_{\text{C}_2\text{H}_2, \text{corr}} = 0.04$  Pa,  $F_{\text{C}_2\text{H}_2} = 14\text{ cm}^3/\text{min}$  at  $I_{\text{arc}} = 0$  A. Besides the usual peaks of the background gas in an analyser belonging to water ( $m/q = 17\text{--}18$  amu), nitrogen ( $m/q = 28$  amu) and  $\text{CO}_2$  ( $m/q = 44$  amu), the spectrum taken before ignition of the discharge contains strong peaks of argon ( $m/q = 40$  and 20 amu) and of parent and fragment ions of  $\text{C}_2\text{H}_2$  ( $m/q = 24\text{--}27$  and 13 amu). The source of hydrogen at  $m/q = 1$  and 2 amu may be either  $\text{C}_2\text{H}_2$  and/or water.

After ignition of the discharge (the same pressure,  $F_{\text{C}_2\text{H}_2} = 34\text{ cm}^3/\text{min}$ ), the spectrum in Fig. 4 b. is greatly changed in the  $\text{C}_2\text{H}_2$ -related peaks, while the intensity of the other

peaks remains basically unchanged. Namely, the peak at the mass number 26 amu ( $C_2H_2$ ) decreases by a factor of about 100 while the hydrogen  $H_2$  peak increases by the same factor. The peaks of  $CH$  ( $m/q = 13$  amu),  $C_2$  ( $m/q = 24$  amu) and  $C_2H$  ( $m/q = 25$  amu) fall below the detection limit. In spite of problems with accurate quantitative interpretation of such measurements, (e.g. the signal of radicals with high sticking coefficient is much suppressed in comparison with, say, argon), the large change in the relation between  $H_2$  and  $C_2H_2$  signal after ignition of the discharge allows to conclude that even during the discharge at moderate arc currents the atmosphere is composed mainly of argon and hydrogen, as a product of acetylene dissociation with some traces of hydrocarbon radicals,  $CH_3$  and  $CH_4$ . As a consequence of the high hydrogen concentration during the discharge, the pressure measured by ion gauge is greatly overestimated. Therefore, the small increase in the acetylene flow with the increasing arc current is due to the decrease in the real pressure.

The acetylene dissociation is proportional to the arc current. The degree of dissociation is very high under the standard evaporation conditions. The hydrocarbons are almost completely stripped of hydrogen leaving mostly  $C^+$ , some radicals  $CH_x^+$  and hydrogen. A high degree of acetylene dissociation in the system can not be explained by one-step electron impact dissociation. The acetylene-related spectra of positive ions are substantially different

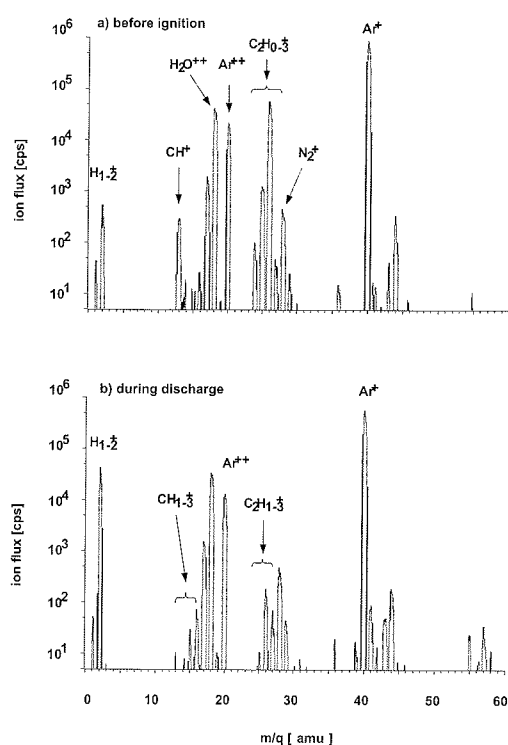


Fig. 4: The mass spectra of neutrals (i.e. using the spectrometer ionisation source) before (a,  $F_{C_2H_2} = 14 \text{ cm}^3/\text{min}$ ) and during discharge (b,  $F_{C_2H_2} = 34 \text{ cm}^3/\text{min}$ ) in an  $Ar/C_2H_2$  working gas mixture.

from the mass spectra of  $C_2H_2$  gas without discharge. Note that even the peak at  $m/q = 6$  amu ( $C^{++}$ ) is present and that the peak at  $m/q = 12$  amu ( $C^+$ ) is the most intense of all hydro-carbon peaks in the spectra of positive ions. It seems quite reasonable, that other reactions within the volume of the plasma, like charge transfer and Penning ionisation/dissociation, also play an important role.

On the other hand the high degree of Ti ionisation into doubly, triply and even higher charged states can be explained by electron impact ionisation,  $Ti^{n+} + e \rightarrow Ti^{(n+1)+} + 2e$ ,  $n = 0-3$ , within the electron beam of a few centimetre and with an electron energy slightly above the threshold for the ionisation of the triply charged Ti ion, i.e. about 27.5 V.

### 3.4 Multiple ion detection

Energy resolved mass spectroscopy is also a viable tool for process monitoring. For this purpose MID technique is used. A very important step before the deposition of any thin film is the cleanness of the substrates. Therefore, a typical deposition process includes a preheating step, as well as ion etching of the substrates without opening of the vacuum chamber.

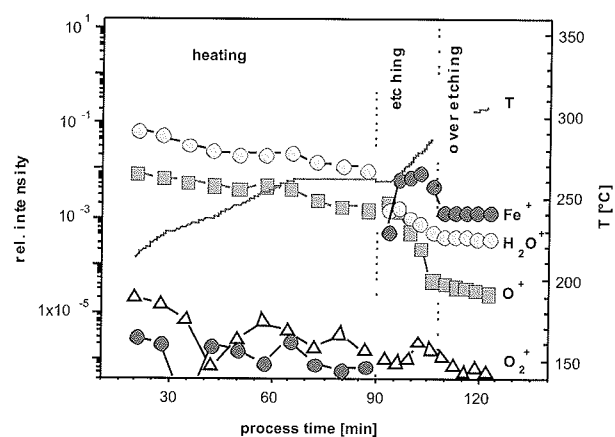


Fig. 5: Relative intensities of significant ions during the heating and etching steps, prior to the ion plating of hard coating

The question is when to terminate etching? An excessively long etching step increases the roughness of the substrates, while inadequately etched substrates suffer on poor adhesion. In Fig. 5 typical example of MID spectra normalized to Ar ions density for heating and etching step is shown. It has to be noted, that the etching time was longer than necessary to show the effect of over-etching. The break in spectra between both steps is due to the change in MID parameters as a result in different energy distributions. As already shown in [6] the energy distribution of ions has peaks ( $E_p$ ) at different values, corresponding to plasma potential.  $E_p$  equals to 15 V for heating, 12 V for etching and 52 V for deposition

From Fig. 5 it is clearly seen that during heating the intensities of  $O^+$ ,  $H_2O^+$  and  $O_2^+$  ions slowly decrease, for less

than one decade per hour. This rate is independent on temperature of dummy stainless steel substrates, which rose to 250°C as measured by TC. During etching, the intensities of  $O^+$  and  $H_2O^+$  ions drop in 15 min for almost two decades. The intensity of  $O_2^+$  ion decreases with the same rate as before. The increase in intensity of  $Fe^+$  ion for 4 decades in first minutes of etching indicates the cleaning of the surface oxide. The native oxide is removed after app. 15 min. This was indicated by the fact that the intensities of  $O^+$ ,  $H_2O^+$  and  $Fe^+$  ions become stable, while the temperature of the substrates gradually rises to above 300°C. Any additional etching increases the surface roughness, and should be avoided.

#### 4. conclusions

Energy resolved mass spectroscopy is a very versatile method for the plasma characterisation. It enables the analysis of *ion energy* distributions of selected ions (and neutrals). Previously published /5/ results show a good correlation between the average energy of the particles bombarding the surface and the properties of the layer (texture, stress free lattice parameter and in minor extend others, like microhardness and internal stress).

Knowing the ion energy, *mass spectra* can be measured. On this way the composition of charged plasma particles and their degree of ionisation can be analysed. Using the ionisation cell the thermal and energetic neutrals can be analysed as well.

*MID techniques* provide real-time information on the process. Substrate cleaning/etching can be terminated exactly at the point, when the surface is clean, without unnecessary over-etching by monitoring  $O^+$ ,  $H_2O^+$  and  $Fe^+$  (substrate) ions. It can be applied to the other plasma assisted processes like etching and plasma cleaning.

#### Acknowledgment

This work was done during my stay at Jožef Stefan Institute and was supported by the Ministry of Higher Education, Sciences and Technology of the Republic of Slovenia.

#### References

- /1/ A. Grill, Cold Plasma in Materials and Fabrication, IEEE Press, NY, 1994
- /2/ N. Herskowitz, Langmuir probe diagnostics, in D.A. Glocker, S. Ismath Shah, (Eds.), Handbook of Thin Film Process Technology, Institute of Physics Publishing, Bristol, 1995, p. D3.0:1.
- /3/ G. Baravian, G. Sultan, E. Damon, H. Detour, C. Hayaud, P. Jacquot, Surf. Coat. Technol., **76-77** (1995) 678-693
- /4/ M. Nesládek, C. Quaeys, S. Wouters, L.M. Stals, E. Bergmann, G. Rettinghaus, Surf. Coat. Technol., **68-69** (1994) 339-343
- /5/ S. Kadlec, M. Maček, S. Kadlec, M. Maček, S. Wouters, B. Meert, B. Navinšek, P. Panjan, C. Quaeys, L. M. Stals, Surf. Coat. Technol., **116-119** (1999) 1211-1218
- /6/ M. Maček, B. Navinšek, P. Panjan, S. Kadlec, Surf. Coat. Technol., **135** (2001) 208-220
- /7/ K.S. Fancey, A. Matthews, Appl. Phys. Lett., **55(9)** (1989) 834-836
- /8/ S. Wouters, S. Kadlec, C. Quaeys, L.M. Stals, Surf. Coat. Technol., **97**, (1997) 114-121
- /9/ S. Wouters, S. Kadlec, C. Quaeys, L.M. Stals, J. Vac. Sci. Technol., **A 16(5)** (1998) 2816-2826
- /10/ S. Wouters, S. Kadlec, M. Nesládek, C. Quaeys, L.M. Stals, Surf. Coat. Technol., **76-77** (1995) 135-141
- /11/ M. Maček, M. Čekada, Surf. Coat. Technol., **180-181** (2004) 2-8
- /12/ M. Maček, M. Mišina, M. Čekada, P. Panjan, Vacuum, **80** (2005) 184-188
- /13/ M. Maček, B. Navinšek, P. Panjan, S. Kadlec, S. Wouters, C. Quaeys, L.M. Stals, Surf. Coat. Technol., **113** (1999) 149-156
- /14/ M. Maček, M. Čekada, M. Mišina, Czechoslovak Journal of Physics, Vol **50**, Suppl. S3 (2000) 403-408
- /15/ A. Buuron, F. Koch, M. Nöthe, H. Bolt, Surf. Coat. Technol., **116** (1999) 755-765

Marijan Maček  
University of Ljubljana, Faculty of Electrical  
Engineering, Tržaška 25,  
1000 Ljubljana, Slovenia

Miha Čekada  
Jožef Stefan Institute, Jamova 39,  
1000 Ljubljana, Slovenia

Prispelo (Arrived): 17.09.2008

Sprejeto (Accepted): 15.12.2008